

## Second Ionization Energies of Gaseous Iron Oxides and Hydroxides: The $\text{FeO}_m\text{H}_n^{2+}$ Dications ( $m = 1, 2$ ; $n \leq 4$ )<sup>†</sup>

Detlef Schröder,\* Susanne Bärsch, and Helmut Schwarz\*

*Institut für Organische Chemie der Technischen Universität Berlin, Strasse des 17. Juni 135, D-10623 Berlin, Germany*

*Received: December 13, 1999; In Final Form: February 29, 2000*

The energetics of selected dicationic iron oxides and hydroxides  $\text{FeO}_m\text{H}_n^{2+}$  ( $m = 1, 2$ ;  $n \leq 4$ ) are probed by charge-stripping mass spectrometry in conjunction with ab initio calculations employing the B3LYP/6-311+G\* level of theory. Specifically,  $\text{Fe}^+$ ,  $\text{FeO}^+$ ,  $\text{FeOH}^+$ ,  $\text{Fe}(\text{H}_2\text{O})^+$ ,  $[\text{Fe}, \text{O}_2, \text{H}_2]^+$ ,  $(\text{H}_2\text{O})\text{FeOH}^+$ , and  $\text{Fe}(\text{H}_2\text{O})_2^+$  and their respective dications are examined. In most cases, reasonable agreement between experiment and theory is found, and discrepancies can be attributed to interferences in the experimental study. Nevertheless, some shortcomings of the theoretical approach are obvious. Combination of experimental and theoretical results leads to adiabatic ionization energies of the monocationic iron compounds:  $\text{IE}_a(\text{FeO}^+) = 18.3 \pm 0.4$  eV,  $\text{IE}_a(\text{FeOH}^+) = 17.0 \pm 0.4$  eV,  $\text{IE}_a(\text{Fe}(\text{H}_2\text{O})^+) = 14.3 \pm 0.5$  eV,  $\text{IE}_a((\text{H}_2\text{O})\text{FeOH}^+) = 15.6 \pm 0.5$  eV, and  $\text{IE}_a(\text{Fe}(\text{H}_2\text{O})_2^+) = 12.6 \pm 0.4$  eV. In the case of  $[\text{Fe}, \text{O}_2, \text{H}_2]^+$ , structural isomerism and isobaric interferences give rise to a composite charge-stripping peak and prevent the experimental determination of the ionization energy. Interestingly, the computational results suggest a reversed order of stabilities for the mono- and dicationic  $[\text{Fe}, \text{O}_2, \text{H}_2]^{+/2+}$  isomers, i.e.,  $\text{Fe}(\text{OH})_2^+ > (\text{H}_2\text{O})\text{FeO}^+ > \text{Fe}(\text{H}_2\text{O}_2)^+ > \text{Fe}(\text{H}_2\text{O})_2^{2+} > (\text{H}_2\text{O})\text{FeO}^{2+} > \text{Fe}(\text{OH})_2^{2+}$ . The ion energetics are used to assess the effects of ligation on the stabilities of the iron dications. While the covalent Fe–O and Fe–OH bonds decrease with increasing oxidation state of the metal, the interactions with water are dominated by electrostatic contributions. On average, solvation by water lowers the second ionization energy of the iron compounds studied by as much as  $1.6 \pm 0.3$  eV

### Introduction

We are currently working on a comprehensive survey of the properties of neutral and charged iron oxides and hydroxides,<sup>1–3</sup> which are of relevance for the redox chemistry of iron in humid or aqueous media, clouds, etc.<sup>4,5</sup> Here, we report the generation of  $\text{FeO}_m\text{H}_n^{2+}$  dications ( $m = 1, 2$ ;  $n \leq 4$ ) by means of charge-stripping (CS) mass spectrometry<sup>6,7</sup> as well as experimental and theoretical results concerning the IEs of the corresponding monocations. In typical CS experiments, monocation precursors are converted to dications in high-energy collisions of the singly charged projectiles with quasi-stationary target gases; in the present case, the monocation kinetic energies are ca. 8000 eV and molecular oxygen serves as collision gas. In such a collision, ionization to the dication can be assumed to occur vertically, and the ionization energy of the monocation  $\text{IE}(\text{M}^+)$  is provided by the kinetic energy of the projectile. This results in a shift of the dication signal on the kinetic energy scale, usually referred to as  $Q_{\min}$  value.<sup>8</sup> To a first approximation,  $Q_{\min}$  corresponds to the vertical ionization energy of the monocation,  $\text{IE}_v(\text{M}^+)$ . Conversion of vertical to adiabatic values,  $\text{IE}_a(\text{M}^+)$ , and valuable insight upon bonding features is gained by complementary ab initio studies.

Specifically, we report CS experiments with  $\text{Fe}^+$ ,  $\text{FeO}^+$ ,  $\text{FeOH}^+$ ,  $\text{Fe}(\text{H}_2\text{O})^+$ ,  $[\text{Fe}, \text{O}_2, \text{H}_2]^+$ ,  $(\text{H}_2\text{O})\text{FeOH}^+$ , and  $\text{Fe}(\text{H}_2\text{O})_2^+$  monocations together with calculations conducted at the B3LYP/6-311+G\* level of theory. Particular attention is paid to experimental aspects, such as calibration schemes, and possible

interferences.  $[\text{Fe}, \text{O}_2, \text{H}_2]^{+/2+}$  deserves a separate discussion, because structural isomers need to be considered,<sup>9</sup> and contributions of isobaric interferences are obvious (see below). Combination of the experimental and theoretical data allows the assessment of the vertical and adiabatic ionization energies of the iron compounds under study. Further, Born–Haber cycles are used to correlate the dication energetics with the corresponding redox properties of the mononuclear iron compounds.<sup>2,10</sup>

### Experimental Methods

The experiments were performed with a modified VG-ZAB/HF/AMD-604 four-sector mass spectrometer of BEBE configuration which has been described elsewhere.<sup>11</sup> Briefly, the  $\text{FeO}_m\text{H}_n^+$  monocations were generated by chemical ionization (CI) of mixtures of  $\text{Fe}(\text{CO})_5$ ,  $\text{N}_2\text{O}$ , and  $\text{H}_2\text{O}$  in which the mixing ratios were adjusted to optimize the ion intensities of interest while minimizing isobaric interferences (see below);  $\text{Fe}(\text{CO})_5$  is always a minor component. Under typical CI conditions, the intensity ratios of the  $\text{FeO}_m\text{H}_n^+$  species were roughly  $\text{FeO}^+ : \text{FeOH}^+ : \text{Fe}(\text{H}_2\text{O})^+ \approx 10:1:8$  for  $m = 1$  and  $[\text{Fe}, \text{O}_2, \text{H}_2]^+ : (\text{H}_2\text{O})\text{FeOH}^+ : \text{Fe}(\text{H}_2\text{O})_2^+ \approx 4:1:5$  for  $m = 2$ , respectively. The species generated in the ion source were characterized by collisional activation (CA) of the B(1)/E(1) mass-selected ions using helium (80% transmission = 80% T) as collision gas. Because of the superior energy resolution of E(1), the energy-resolved CS experiments were conducted with B(1)-only mass-selected ions.<sup>2,10,12</sup> To this end, the mono- and dication signals in charge-stripping experiments were scanned at energy resolutions  $E/\Delta E \geq 4000$ , and the  $Q_{\min}$  values were determined from the

<sup>†</sup> Dedicated to Professor Vladimir Bondybey on the occasion of his 60th birthday.

**TABLE 1: Measured  $Q_{\min}$  Values (in eV) for Charge Stripping of Mass-Selected  $\text{FeO}_m\text{H}_n^+$  Monocations to the Corresponding Dications Determined in Several Independent Experiments 1–8 and the Derived Averages<sup>a</sup>**

precursor	1	2	3	4	5	6	7	8	mean
$\text{Fe}^+$	15.40	15.19	15.73	15.23					$15.39 \pm 0.25$
$\text{FeO}^+$	18.56	18.95	18.83	18.77	18.24	18.26	18.64	18.76	$18.63 \pm 0.26$
$\text{FeOH}^+$	17.11	17.06	17.39	16.92	17.67	17.23	17.54	17.47	$17.30 \pm 0.26$
$\text{Fe}(\text{H}_2\text{O})^+$	14.08	14.45	14.75	14.78	14.54	14.37	14.07	14.23	$14.41 \pm 0.28$
$[\text{Fe}, \text{O}_2, \text{H}_2]^+$	13.98	14.06	13.55	12.36	14.10	13.65	15.05	14.70	$13.93 \pm 0.81$
$(\text{H}_2\text{O})\text{FeOH}^+$	15.38	16.08	15.74	16.37	15.64				$15.84 \pm 0.39$
$\text{Fe}(\text{H}_2\text{O})_2^+$	12.25	12.86	12.35	12.81	12.87				$12.63 \pm 0.30$

<sup>a</sup> For the sake of consistency, multiplicative corrections are employed throughout.

difference between the high-energy onsets of the mono- and the dication peaks.<sup>13,14</sup> Due to hardware limitations, these spectra were recorded as superposition of single scans using an  $x/y$  recorder in order to maintain the full energy resolution of the instrument. The monocation signals were carefully focused to symmetric Gaussian-type peak shapes in the absence of collision gas. In the presence of collision gas, both mono- and dication signals showed typical low-energy tails due to collisional broadening. Calibration of the kinetic energy scale applied charge stripping of the molecular ion of toluene,  $\text{C}_7\text{H}_8^+ \rightarrow \text{C}_7\text{H}_8^{2+}$  with  $Q_{\min}(\text{C}_7\text{H}_8^+) = 15.7$  eV,<sup>6–8</sup> using both additive and multiplicative schemes<sup>8</sup> as discussed further below. The values given are averages of at least four different experiments, and the indicated errors comprise one standard deviation. Note that the determination of  $Q_{\min}$  values relies on four separate energy-resolved measurements, i.e., the mono- and dication signals of interest and the mono- and dications of toluene ion serving as a reference. Each of these experiments is sensitive to accidental changes in the ionization conditions (discharges in particular), while the evaluation of  $Q_{\min}$  data requires the constancy of the absolute ion kinetic energies in all four measurements. Hence, repetitive measurements are mandatory, and extreme deviations were discarded in the data evaluation.

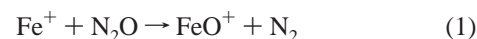
### Theoretical Methods

For the computational study of singly and doubly charged  $\text{FeO}_m\text{H}_n^{+/2+}$ , we employed the B3LYP functional implemented in Gaussian94 together with 6-311+G\* basis sets.<sup>15</sup> The B3LYP approach has recently been demonstrated to yield a reasonably accurate description of gaseous iron compounds.<sup>16</sup> Rather than providing a set of ab initio thermochemical data for  $[\text{Fe}, \text{O}_m, \text{H}_n]^{+/2+}$ , the primary aim of our theoretical investigation is the assessment of the differences between the vertical and adiabatic ionization energies of the species under study. In this respect, choice of the B3LYP/6-311+G\* level of theory appears as a reasonable compromise. The accuracy of the absolute energetics is addressed further below.

The calculations follow the scheme outlined next. First, the monocationic species were fully optimized on the respective low- and high-spin surfaces, where the choice of electronic states to be considered was guided by literature studies of these and related systems (see below). Then, vertical ionization energies were determined for each low-lying spin state by calculating the dications at the respective monocation geometries. Finally, the lowest lying states of the dications were geometry-optimized in order to determine the differences between adiabatic and vertical ionization energies. Even though all geometry-optimized species were characterized as minima by means of frequency calculations, zero-point vibrational energies are generally not included in the data given below, because this appears inappropriate in the comparison of vertical and adiabatic properties.

### Experimental Results

The  $\text{FeO}_m\text{H}_n^+$  cations of interest in this study can be generated by chemical ionization (CI) of mixtures of  $\text{Fe}(\text{CO})_5$ ,  $\text{N}_2\text{O}$ , and  $\text{H}_2\text{O}$ . In the CI plasma, a manifold of reactions occur after (dissociative) ionization of  $\text{Fe}(\text{CO})_5$ , either directly or, more likely, via charge transfer with ionized  $\text{N}_2\text{O}$  and/or  $\text{H}_2\text{O}$  as major components of the CI mixtures used. Starting from bare  $\text{Fe}^+$ , the  $\text{FeO}^+$  cation can be formed with  $\text{N}_2\text{O}$  according to reaction 1.<sup>17</sup> The iron hydroxide  $\text{FeOH}^+$  may arise from either reaction



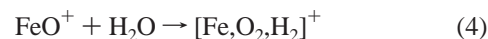
2a and/or 2b which are both endothermic,<sup>18</sup> but nevertheless



occur in the CI plasma to some extent. The iron–water complex  $\text{Fe}(\text{H}_2\text{O})^+$  is most likely generated via ligand exchange according to reaction 3.<sup>21</sup> The  $\text{FeO}_2\text{H}_n^+$  cations can then be regarded



as association products of these primary ions (reactions 4–6).<sup>3,22,23</sup>



In addition, efficient formation of  $[\text{Fe}, \text{O}_2, \text{H}_2]^+$  has been reported in the reaction of  $\text{Fe}(\text{H}_2\text{O})^+$  with  $\text{N}_2\text{O}$ .<sup>24</sup>

While various other routes are conceivable to occur in the CI plasma, in the present context it is sufficient to state that CI of  $\text{Fe}(\text{CO})_5/\text{N}_2\text{O}/\text{H}_2\text{O}$  mixtures allows generation of the ions of interest in reasonable amounts and purities; the latter were assessed by the collisional activation spectra of the mass-selected monocations (not shown), which were consistent with the designated formula, unless mentioned otherwise. In this contribution, we almost exclusively address the  $Q_{\min}$  values determined for the monocations generated in the CI plasma, paying particular attention to several experimental aspects. As an illustration of the experimental data, Table 1 shows the  $Q_{\min}$  values obtained in several independent experiments and the resulting averages. While there exist two different calibration schemes in charge-stripping measurements,<sup>8</sup> we concentrate on the multiplicative correction method throughout in this section; comparison to the additive calibration scheme is made where appropriate in the discussion.

**$\text{Fe}^{+/2+}$ .** Mass selection of  $\text{Fe}^+$  cations generated under CI conditions and subsequent energy-resolved charge stripping

provides  $Q_{\min}(\text{Fe}^+) = 15.39 \pm 0.25$  eV (Table 1). The measured value is clearly outside the error margins of the spectroscopic reference  $\text{IE}(\text{Fe}^+) = 16.1879 \pm 0.0012$  eV.<sup>25</sup> In contrast, previous charge-stripping experiments of McCullough-Catalano and Lebrilla<sup>14</sup> gave  $Q_{\min}(\text{Fe}^+) = 16.3 \pm 0.4$  eV. Underestimation of  $Q_{\min}(\text{Fe}^+)$  in our experiments indicates the presence of excited states in the beam of mass-selected  $\text{Fe}^+$  monocations.<sup>7</sup> This is in fact quite conceivable as dissociative ionization of  $\text{Fe}(\text{CO})_5$  is known to generate significant amounts of electronically excited  $\text{Fe}^+$  cations.<sup>26</sup> The observed shift between our measured  $Q_{\min}(\text{Fe}^+) = 15.39 \pm 0.25$  eV and  $\text{IE}(\text{Fe}^+) = 16.1879 \pm 0.0012$  eV is mostly consistent with contribution of excited  $\text{Fe}^+$  ( $^4\text{D}$ ) to the precursor beam which lies 0.98 eV above the  $\text{Fe}^+$  ( $^6\text{D}$ ) ground state. Reproduction of the spectroscopic value by McCullough-Catalano and Lebrilla<sup>14</sup> can be attributed to their use of fast atom bombardment (FAB) as ionization method which is known to be a softer ionization technique than electron ionization and often leads to the formation of atomic ions in their ground states.<sup>27</sup> Interestingly, also  $\text{Fe}^+$  generated by dissociative electron ionization of ferrocene has been reported to reproduce the spectroscopic  $\text{IE}(\text{Fe}^+)$  within experimental error.<sup>28</sup>

The presence of electronically excited states in the monocation beams could also affect the  $Q_{\min}$  data of the molecular species addressed. Rovibronic excitation of the monocation precursors is less severe because it is likely to be mapped onto the dication surface upon vertical ionization and — to a first approximation — the differential shapes of the mono- and dication surfaces are accounted for in the correction from vertical to adiabatic ionization energies using theoretical data. Electronic excitations of the monocations have dramatic effects, however, because ionization of excited monocations is energetically easier than that of the ground states by the amount of the state splitting (provided that the dication ground state is accessible from both monocation states). In this respect, it is particularly important that the cross section of charge stripping drastically decreases with increasing ionization energy.<sup>29</sup> As a consequence, even minor contributions of electronically excited monocations in the precursor beam can result in substantially underestimated  $Q_{\min}$  values,<sup>30</sup> for which  $\text{Fe}^+$  generated by CI of  $\text{Fe}(\text{CO})_5/\text{N}_2\text{O}/\text{H}_2\text{O}$  is an example. Notwithstanding, we have no indications for the presence of excited states for the  $\text{FeO}_m\text{H}_n^+$  cations examined in this work (see below) and assume that these undergo efficient thermalization in the CI plasma. In contrast, it is precisely the bare metal cation that is likely to experience less thermalization in the plasma compared to  $\text{FeO}_m\text{H}_n^+$  species under study. Thus,  $\text{Fe}^+$  is formed as a primary product of the dissociative ionization of  $\text{Fe}(\text{CO})_5$ , which is known to yield excited cations. While quenching to the ground state might occur in the CI plasma,  $\text{Fe}^+$  is also consumed in reactions with the CI components (e.g., reactions 1 and 2a). In contrast, the generation of the  $\text{FeO}_m\text{H}_n^+$  ions requires the occurrence of ion/molecule reactions in the source; therefore these ions are more likely to undergo thermalizing collisions. As a consequence, contributions of excited states are more likely for  $\text{Fe}^+$  than for the  $\text{FeO}_m\text{H}_n^+$  species extracted from the CI source.

$\text{FeO}^{+2+}$ . Mass-selected  $\text{FeO}^+$  cation yields  $Q_{\min}(\text{FeO}^+) = 18.63 \pm 0.26$  eV, which is consistent with a previous figure of  $Q_{\min}(\text{FeO}^+) = 18.3 \pm 0.3$  eV.<sup>2</sup> While it is possible that slightly different populations of  $\text{FeO}^+$  monocation states were sampled in these experiments, both values are comparable within experimental error. In the present context, let us prefer the higher value determined in the same set of experiments as for the other  $\text{FeO}_m\text{H}_n^+$  ions.<sup>31</sup> The  $Q_{\min}$  value of  $\text{FeO}^+$  is not affected by

changing the  $\text{Fe}(\text{CO})_5/\text{N}_2\text{O}$  ratios, the overall pressure, addition of methane, etc., while notable deviations to lower  $Q_{\min}$  values occur upon admixture of high partial pressures of water to the CI plasma. These can be attributed to an interference of  $^{56}\text{FeO}^+$  by isobaric  $^{54}\text{Fe}(\text{H}_2\text{O})^+$  (both 72 amu); the latter ion has a much smaller ionization energy than  $\text{FeO}^+$  (see below). Contribution of  $^{54}\text{Fe}(\text{H}_2\text{O})^+$  is also obvious from the significant  $^{54}\text{Fe}^+$  signals observed in the CA spectrum of the 72 amu ions generated at higher water pressures.

$\text{FeOH}^{+2+}$ . The experiments yield  $Q_{\min}(\text{FeOH}^+) = 17.30 \pm 0.26$  eV, which is consistent with the (additive) value of  $17.0 \pm 0.4$  eV determined by McCullough-Catalano and Lebrilla.<sup>14</sup> Near-perfect agreement is achieved if the different calibration schemes are taken into account; i.e., using the additive method, we arrive at  $Q_{\min}(\text{FeOH}^+) = 17.03 \pm 0.23$  eV. Notable deviations to higher  $Q_{\min}$  values were found if partial pressures of water were too low, i.e., hardly any  $^{56}\text{FeOH}^+$  is formed, while reaction 1 can still yield isobaric  $^{57}\text{FeO}^+$  (both 73 amu). Further confidence to the measured figure is given by the fact that no changes in  $Q_{\min}$  are observed upon CI of an  $\text{Fe}(\text{CO})_5/\text{N}_2\text{O}/\text{CH}_4$  mixture which is known to serve as an efficient source for  $\text{FeOH}^+$  cation.<sup>23,32</sup>

$\text{Fe}(\text{H}_2\text{O})^{+2+}$ . The  $Q_{\min}$  measurements of this ion are nicely reproducible independent of ionization conditions and lead to  $Q_{\min}(\text{Fe}(\text{H}_2\text{O})^+) = 14.41 \pm 0.28$  eV. The low magnitude of this value provides a clue for the robustness against variations of the experimental conditions because conceivable isobaric interferences, e.g.,  $\text{Fe}^{18}\text{O}^+$  and  $^{57}\text{FeOH}^+$ , have much larger IEs (see above). Though the CI plasma cannot warrant to sample equilibrated species only, we exclude participation of isomeric species such as the insertion intermediate  $\text{HFeOH}^+$  because irrespective of spin-state considerations, several ab initio studies predict this isomer to be considerably less stable than  $\text{Fe}(\text{H}_2\text{O})^+$  while the barrier for hydrogen migration is low.<sup>33–35</sup>

$[\text{Fe}, \text{O}_2, \text{H}_2]^{+2+}$ . The composition of this ion leaves some ambiguity as far as the ion connectivity is concerned. Considering the mode of ion generation in the  $\text{Fe}(\text{CO})_5/\text{N}_2\text{O}/\text{H}_2\text{O}$  plasma, at least iron dihydroxide,  $\text{Fe}(\text{OH})_2^+$ , and hydrated iron oxide,  $(\text{H}_2\text{O})\text{FeO}^+$ , appear conceivable.<sup>3</sup> The detailed aspects of the potential-energy surface of the monocation will be published elsewhere,<sup>9</sup> but for the time being let us concentrate on the dications. The  $Q_{\min}$  value of  $13.93 \pm 0.81$  determined for mass-selected  $[\text{Fe}, \text{O}_2, \text{H}_2]^+$  shows a notably increased spread with the extremes ranging from 12.36 to 15.05 eV. One may attribute this spread to variations in the contributions of the different isomers, having different  $Q_{\min}$  values, to the monocation precursor beam. However, notable  $^{54}\text{Fe}^+$  fragments are observed in the CA mass spectra of the monocations, particularly in those experiments which gave the lowest  $Q_{\min}$  values, thus indicating isobaric interference of  $[\text{Fe}, \text{O}_2, \text{H}_2]^+$  by  $^{54}\text{Fe}(\text{H}_2\text{O})_2^+$  (both 90 amu), of which the latter has a rather small  $Q_{\min}$  value (see below). In fact, the charge-stripping peak obtained at increased energy resolution (Figure 1, upper trace) is composed of two features as becomes obvious from the comparison with the peak obtained for genuine  $^{56}\text{Fe}(\text{H}_2\text{O})_2^+$  (lower trace in Figure 1). Attempts to deconvolute the composite peak indicate that at least three different processes contribute to the charge-stripping peak of the ions at 90 amu. For the time being, let us postpone this topic to the Discussion section after having also considered the computational results for  $[\text{Fe}, \text{O}_2, \text{H}_2]^{+2+}$  mono- and dications.

$(\text{H}_2\text{O})\text{FeOH}^{+2+}$ . Although formed in only moderate amounts upon CI of  $\text{Fe}(\text{CO})_5/\text{N}_2\text{O}/\text{H}_2\text{O}$  mixtures, this ion appears to lack isobaric interferences by iron-containing cations, and

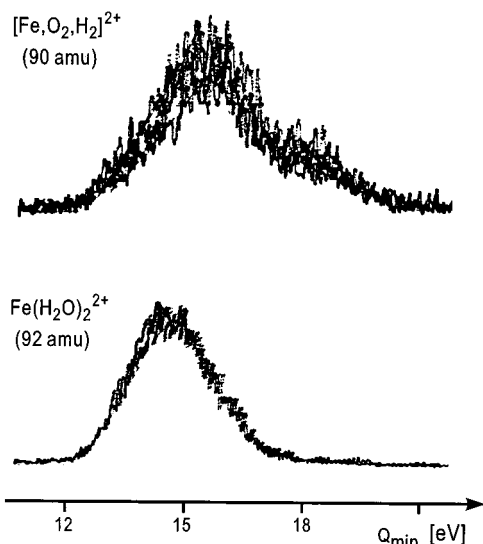


**Figure 1.** Upper trace: energy resolved charge-stripping signal of B(1)-selected  $^{56}\text{Fe}, \text{O}_2, \text{H}_2^+$  ions interfered by isobaric  $^{54}\text{Fe}(\text{H}_2\text{O})_2^+$  (both 90 amu); collision gas: oxygen, 80% T. The spectrum is a superposition of seven single scans recorded with an  $x/y$  recorder. Lower trace: energy resolved charge-stripping signal of B(1)-selected  $^{56}\text{Fe}(\text{H}_2\text{O})_2^+$  (92 amu) recorded in the same series of experiments under identical conditions (three scans superimposed). The  $Q_{\min}$  scale given is approximate.

$Q_{\min}(\text{H}_2\text{O})\text{FeOH}^+ = 15.84 \pm 0.39$  is obtained. In this particular case, however, the proximity of the  $Q_{\min}$  value to that of isobaric  $\text{C}_7\text{H}_7^+$  ( $Q_{\min}(\text{C}_7\text{H}_7^+) = 15.7$  eV),<sup>36</sup> formed from the toluene calibrant, could imply some overlap because mass selection is done with B(1) only. This conjecture can be excluded for several reasons: (i) No typical fragments of  $\text{C}_7\text{H}_7^+$ , e.g.,  $\text{C}_5\text{H}_5^+$ , are observed in the CA spectrum of mass selected  $(\text{H}_2\text{O})\text{FeOH}^+$ . (ii) Interference of  $(\text{H}_2\text{O})\text{FeOH}^+$  (90.949 amu) by  $\text{C}_7\text{H}_7^+$  (91.042 amu) would mean that the latter has a lower kinetic energy. Specifically, if the kinetic energy of  $(\text{H}_2\text{O})\text{FeOH}^+$  is adjusted to the typical value of 7993 eV, transmission of the heavier  $\text{C}_7\text{H}_7^+$  species through B(1) occurs at a kinetic energy of only 7985 eV. Hence, even if some  $\text{C}_7\text{H}_7^+$  contributes to the B(1)-selected beam, it would not affect the high-energy onset of the dication signal. (iii) Relative  $Q_{\min}$  values determined in the absence of the toluene calibrant were consistent with those determined for the other  $\text{FeO}_m\text{H}_n^+$  ions under study. Hence, the measured  $Q_{\min}$  value is assigned to  $(\text{H}_2\text{O})\text{FeOH}^+$ , and the similarity to  $Q_{\min}(\text{C}_7\text{H}_7^+)$  is considered as a mere coincidence.

**$\text{Fe}(\text{H}_2\text{O})_2^{+2+}$ .** Similar to the  $\text{Fe}(\text{H}_2\text{O})^+$  cation, the bisligated  $\text{Fe}(\text{H}_2\text{O})_2^+$  complex yields nicely reproducible results, independent of the ionization conditions, and  $Q_{\min}(\text{Fe}(\text{H}_2\text{O})_2^+) = 12.63 \pm 0.30$  is obtained. Even though interference by  $\text{C}_7\text{H}_8^+$  stemming from the calibrant (both 92 amu) is conceivable, it cannot affect the result considering the arguments raised above for  $(\text{H}_2\text{O})\text{FeOH}^+$  and the fact that the  $Q_{\min}$  value of the toluene reference ion (15.7 eV) is much too large to affect the high-energy threshold of the charge-stripping peak to any notable extent. Further, the energy-resolved charge-stripping signal of  $\text{Fe}(\text{H}_2\text{O})_2^+$  has no indications of an overlapping component (lower trace in Figure 1).

## Theoretical Results

For a computational description of the  $\text{FeO}_m\text{H}_n^{+2+}$  species we have chosen the B3LYP/6-311+G\* level of theory. Clearly, this level is by no means sufficient for an adequate description of the absolute energetics and is known to be subject to various errors in the description of open-shell systems. Nevertheless,

**TABLE 2: Total Energies ( $E_{\text{SCF}}$ , in hartrees), Ionization Energies of  $\text{FeO}_m\text{H}_n^+$  Monocations (IE, in eV), and Offsets between Vertical and Adiabatic Transitions ( $\Delta\text{IE}_{\text{v/a}}$ , in eV) Calculated at the B3LYP/6-311+G\* Level of Theory for  $\text{FeO}_m\text{H}_n^{+2+}$  Mono- and Dications**

	charge	type <sup>a</sup>	spin	$E_{\text{SCF}}^b$	IE	$\Delta\text{IE}_{\text{v/a}}$
Fe	+2		5	-1262.7492	16.52	
	+1		6	-1263.3563		
	+2		5	-1262.7492	16.70	
	+1		4	-1263.3630		
FeO	+2	sp(6)	5	-1337.8771	18.93	0.18
	+2	opt	5	-1337.8837	18.75	
	+1	opt	6	-1338.5727		
	+1	opt	4	-1338.5597		
FeOH	+2	sp(5)	4	-1338.6075	17.63	0.35
	+2	opt	4	-1338.6204	17.28	
	+2	sp(5)	6	-1338.6224	17.23	0.33
	+2	opt	6	-1338.6344	16.90	
	+1	opt	5	-1339.2554		
	+1	opt	3	-1339.1936		
Fe(H <sub>2</sub> O)	+2	sp(4)	5	-1339.3527	14.25	0.02
	+2	opt	5	-1339.3532	14.23	
	+1	opt	4	-1339.8763		
	+2	sp(6)	5	-1339.3458	14.04	0.20
Fe(OH) <sub>2</sub>	+2	opt	5	-1339.3532	13.84	
	+1	opt	6	-1339.8617		
	+2	sp(6)	5	-1414.4656	17.87	0.35
	+2	opt	5	-1414.4787	17.52	
(H <sub>2</sub> O)FeO	+1	opt	6	-1415.1223		
	+1	opt	4	-1415.1005		
	+2	sp(6)	5	-1414.4757	17.02	0.20
	+2	opt	5	-1414.4831	16.82	
Fe(H <sub>2</sub> O) <sub>2</sub>	+2	sp(6)	3	-1414.4673		
	+1	opt	6	-1415.1012		
	+1	opt	4	-1415.0934		
	+2	sp(4)	5	-1414.4843	14.39	0.38
(H <sub>2</sub> O)FeOH	+2	opt	5	-1414.4990	13.99	
	+1	opt	4	-1415.0132		
	+2	sp(6)	5	-1414.4779	14.03	0.57
	+2	opt	5	-1414.4990	13.46	
	+1	opt	6	-1414.9936		
	+2	sp(5)	4	-1415.1945	16.07	0.27
Fe(H <sub>2</sub> O) <sub>2</sub>	+2	opt	4	-1415.2047	15.80	
	+1	opt	5	-1415.7852		
	+1	opt	3	-1415.7178		
	+2	sp(4)	5	-1415.9280	12.46	0.04
Fe(H <sub>2</sub> O) <sub>2</sub>	+2	opt	5	-1415.9295	12.42	
	+1	opt	4	-1416.3860		
	+1	opt	6	-1416.3354		

<sup>a</sup> sp, single-point calculation of the dication at the geometry of the monocation, spin state indicated in parentheses; opt, fully geometry optimized dication of given multiplicity. <sup>b</sup> 1 hartree = 27.2116 eV.

B3LYP performs quite favorably for transition-metal compounds<sup>37–39</sup> including those of iron.<sup>16</sup> Moreover, the main concern of the present study is relative energies, i.e., those of possible structural and/or electronic isomers for a given charge state and those between the mono- and dications. The differences of vertical and adiabatic ionization energies of the monocations from those of the dications are of particular relevance for the conversion of the experimental  $Q_{\min}$  values to thermochemical data. In this respect, the B3LYP approach offers a good compromise between the accuracy of the description and the computational costs. Table 2 gives the computed total energies of all species studied with this approach.

**$\text{Fe}^{+2+}$ .** Many computational approaches using density functional theory, of which B3LYP is a variant, tend to prefer low- vs high-spin states due to overestimation of correlation energy. In fact, B3LYP/6-311+G\* predicts the low-spin state  $\text{Fe}^+$  (<sup>4</sup>F) as 0.18 eV more stable than  $\text{Fe}^+$  (<sup>6</sup>D), while the latter is the ground state of iron cation with a splitting of 0.25 eV to the  $\text{Fe}^+$  (<sup>4</sup>F) quartet state.<sup>25</sup> Overall, this means that the B3LYP

approach is in error by about 0.4 eV for the bare atom. Errors of similar size have been found in several other B3LYP studies of iron compounds, and often an uncertainty of  $\pm 0.5$  eV is assigned to this approach.<sup>10,16,37,40,41</sup>

As far as ionization to dications is concerned, the effect on the monocation coincides with a slight destabilization of the  $\text{Fe}^{2+}$  ( $^5\text{D}$ ) dication for the very same reason, therefore leading to an overestimation of  $\text{IE}(\text{Fe}^+, \text{calc}) = 16.52$  eV in comparison to the spectroscopic value of  $\text{IE}(\text{Fe}^+) = 16.19$  eV.<sup>25</sup> For the transition  $\text{Fe}^+$  ( $^4\text{F}$ )  $\rightarrow$   $\text{Fe}^{2+}$  ( $^5\text{D}$ ), the erroneous ground-state assignment with B3LYP leads to  $\text{IE}(\text{Fe}^+(\text{4F}), \text{calc.}) = 16.70$  eV compared to the experimental IE of only 16.01 eV for  $\text{Fe}^+$  ( $^4\text{F}$ ). These deviations between spectroscopic data of the atom and the theoretical values may serve as a guide for the assessment of the absolute accuracy of the computational predictions. Nevertheless, note that the computational errors of the molecular ions are expected to be somewhat smaller, as the effect of the overestimation of the low-spin species is most pronounced for atomic ions.

**$\text{FeO}^{+/2+}$ .** While the accurate theoretical description of bare  $\text{Fe}^+$  is already difficult, the  $\text{FeO}^+$  cation belongs to the most challenging problems among small 3d-metal compounds. The Fe–O bond in  $\text{FeO}^+$  is highly polarized and has significant multireference character. Notwithstanding, all computational studies made so far agree upon a  $^6\Sigma^+$  ground state of  $\text{FeO}^+$  even though the calculated state splittings diverge;<sup>33–35,42,43</sup> recent experimental data further support the sextet ground state.<sup>44</sup> For the dication, we considered the quintet  $\text{FeO}^{2+}$  ( $\Delta^5$ ) predicted by Yoshizawa et al.<sup>43</sup> Our B3LYP calculations predict  $\text{IE}_v(\text{FeO}^+) = 18.93$  eV and  $\text{IE}_a(\text{FeO}^+) = 18.75$  eV, respectively. The offset between vertical and adiabatic ionization energies,  $\Delta\text{IE}_{v/a} = 0.18$  eV, can be attributed to the different bond lengths, i.e.,  $r_{\text{Fe–O}} = 1.64$  Å in the monocation and 1.83 Å in the dication (Figure 2). However, the difference is much smaller than  $\Delta\text{IE}_{v/a} = 0.6 \pm 0.1$  eV estimated in our previous study based on the analogy to the related  $\text{FeS}^{+/2+}$  system.<sup>2</sup> Note, however, that we have not considered other spin states of  $\text{FeO}^{2+}$ , such as the low-lying triplet and septet states that matter in the case of  $\text{FeS}^{2+}$  dication,<sup>2</sup> simply because B3LYP does not allow an unambiguous assignment of the ground state of the  $\text{FeO}^{2+}$  dication.

**$\text{FeOH}^{+/2+}$ .** Previous computational studies have predicted a quintet ground state for iron hydroxide cation.<sup>16,34</sup> According to our calculations, triplet  $\text{FeOH}^+$  is 1.68 eV higher in energy and therefore not considered any further. Ionization of the quintet to the dication surface results in  $\text{IE}_v(\text{FeOH}^+) = 17.23$  eV as well as  $\text{IE}_a(\text{FeOH}^+) = 16.90$  eV and thus  $\Delta\text{IE}_{v/a} = 0.33$  eV. Interestingly, the major source for the offset is the bond angle which changes from  $\alpha_{\text{FeOH}} = 154^\circ$  in  $\text{FeOH}^+$  to a practically linear arrangement in the sextet ground state of the dication, whereas  $r_{\text{Fe–O}}$  remains virtually unchanged. In a simple bonding scheme, the linear arrangement of  $\text{FeOH}^{2+}$  can be understood as protonation of  $\text{FeO}^+$  ( $^6\Sigma^+$ ) at an oxygen-centered  $\sigma$ -type orbital. As with the isoelectronic  $\text{FeO}^+$ , a low-lying quartet state exists for  $\text{FeOH}^{2+}$ . Consistent with the bonding mnemonic of the sextet, the quartet state of  $\text{FeOH}^{2+}$  is bent ( $r_{\text{Fe–O}} = 1.92$  Å,  $r_{\text{O–H}} = 1.00$  Å,  $\alpha_{\text{FeOH}} = 160^\circ$ ). Elongation of  $r_{\text{Fe–O}}$  in the dication gives rise to  $\Delta\text{IE}_{v/a} = 0.35$  eV for the transition  $\text{FeOH}^+$  ( $^5\text{A}'$ )  $\rightarrow$   $\text{FeOH}^{2+}$  ( $^4\text{A}'$ ). Whether or not the B3LYP assignment of the quartet/sextet splitting is correct, the similar  $\Delta\text{IE}_{v/a}$  values predicted for both states permit a straightforward adjustment of the experimental  $Q_{\text{min}}$  value to from  $\text{IE}_v$  to  $\text{IE}_a$ .

**$\text{Fe}(\text{H}_2\text{O})^{+/2+}$ .** As with bare  $\text{Fe}^+$ , density functional methods encounter a spin problem also in the case of the  $\text{Fe}(\text{H}_2\text{O})^+$  complex. Our prediction is a  $^4\text{A}_2$  ground state<sup>34,35</sup> while high-

level ab initio methods clearly prefer a sextet state ( $^6\text{A}_1$ ).<sup>35,45</sup> Similarly, the B3LYP results show an overestimated stability of the quartet species. For the  $\text{Fe}(\text{H}_2\text{O})^{2+}$  dication, a quintet ground state is predicted by B3LYP. For the transition  $\text{Fe}(\text{H}_2\text{O})^+$  ( $^6\text{A}_1$ )  $\rightarrow$   $\text{Fe}(\text{H}_2\text{O})^{2+}$  ( $^5\text{A}_1$ ), we obtain  $\text{IE}_v(\text{Fe}(\text{H}_2\text{O})^+) = 14.04$  eV,  $\text{IE}_a(\text{Fe}(\text{H}_2\text{O})^+) = 13.84$  eV, and thus  $\Delta\text{IE}_{v/a} = 0.20$  eV, while  $\text{IE}_v(\text{Fe}(\text{H}_2\text{O})^+) = 14.25$  eV,  $\text{IE}_a(\text{Fe}(\text{H}_2\text{O})^+) = 14.23$  eV, and  $\Delta\text{IE}_{v/a} = 0.02$  eV are obtained for  $\text{Fe}(\text{H}_2\text{O})^+$  ( $^4\text{A}_2$ )  $\rightarrow$   $\text{Fe}(\text{H}_2\text{O})^{2+}$  ( $^5\text{A}_1$ ). The different offsets between vertical and adiabatic transitions for the low- and high-spin species are consistent with the associated changes in geometry. The geometries of  $\text{Fe}(\text{H}_2\text{O})^+$  ( $^4\text{A}_2$ ) and  $\text{Fe}(\text{H}_2\text{O})^{2+}$  ( $^5\text{A}_1$ ) are close to each other, thus resulting in a negligible  $\Delta\text{IE}_{v/a}$ , whereas  $r_{\text{Fe–O}}$  is significantly larger in the high-spin monocation  $\text{Fe}(\text{H}_2\text{O})^+$  ( $^6\text{A}_1$ ) than in the corresponding dication. The failure to reproduce the correct monocation ground state and the ambiguity associated with respect to the  $\Delta\text{IE}_{v/a}$  value to be applied to the experimental  $Q_{\text{min}}$  slightly adds to the uncertainty in the evaluation of the thermochemistry of  $\text{Fe}(\text{H}_2\text{O})^{2+}$  dication to be discussed further below.

**$[\text{Fe}, \text{O}_2, \text{H}_2]^{+/2+}$ .** For this elemental composition, at least three different structural isomers need to be considered: the iron dihydroxides  $\text{Fe}(\text{OH})_2^{+/2+}$ , the water complexes of ionized iron oxide  $(\text{H}_2\text{O})\text{FeO}^{+/2+}$ , and the iron complexes of hydrogen peroxide  $\text{Fe}(\text{H}_2\text{O}_2)^{+/2+}$ . A comprehensive discussion of the energetic and geometrical features of the potential-energy surface of  $[\text{Fe}, \text{O}_2, \text{H}_2]^+$  monocations also including possible insertion isomers will be published elsewhere.<sup>9</sup> For the singly charged ions, B3LYP predicts  $\text{Fe}(\text{OH})_2^+$  as global minimum with  $(\text{H}_2\text{O})\text{FeO}^+$  and  $\text{Fe}(\text{H}_2\text{O}_2)^+$  being 0.57 and 2.96 eV less stable. Similar to  $\text{FeO}^+$ , low-lying quartet states are found for  $\text{Fe}(\text{OH})_2^+$  and  $(\text{H}_2\text{O})\text{FeO}^+$ , but given the tendency of overestimation the stabilities of low-spin states with B3LYP (see above), the assignment of high-spin ground states for these  $[\text{Fe}, \text{O}_2, \text{H}_2]^+$  species seems justified.<sup>46</sup> For the  $\text{Fe}^{+/2+}$  complexes of hydrogen peroxide on the monocation surfaces, quartet and sextet minima of  $\text{Fe}(\text{H}_2\text{O}_2)^+$  are found, but irrespective of spin state these are predicted to be much less stable than the two other  $[\text{Fe}, \text{O}_2, \text{H}_2]^+$  isomers mentioned above. Moreover, the vibrational frequencies associated with the modes corresponding to insertion of the metal into the O–O bond to yield  $\text{Fe}(\text{OH})_2^+$  are on the order of only 100  $\text{cm}^{-1}$ , suggesting facile interconversion of  $\text{Fe}(\text{H}_2\text{O}_2)^+$  to the more stable isomers.<sup>47</sup> Interestingly, the situation is inverse for the dications. Here,  $\text{Fe}(\text{H}_2\text{O}_2)^{2+}$  is predicted to form the global minimum, whereas  $(\text{H}_2\text{O})\text{FeO}^{2+}$  is 0.43 eV and  $\text{Fe}(\text{OH})_2^{2+}$  even 0.55 eV higher in energy. This change of stability order from the mono- to the dication surfaces can be attributed to the avoidance of high valencies at the metal center; i.e., formal iron(II) in  $\text{Fe}(\text{H}_2\text{O}_2)^{2+}$  is preferred over iron(IV) in  $(\text{H}_2\text{O})\text{FeO}^{2+}$  and  $\text{Fe}(\text{OH})_2^{2+}$ ; a similar effect is operative in the  $\text{FeCl}_2^{+/2+}/\text{Fe}(\text{Cl}_2)^{+/2+}$  couple of isomers.<sup>10</sup>

The variation in mono- and dication stabilities of the different isomers give a set of ionization energies which range from 13.46 eV for the adiabatic transition  $\text{Fe}(\text{H}_2\text{O}_2)^+$  ( $^6\text{A}$ )  $\rightarrow$   $\text{Fe}(\text{H}_2\text{O}_2)^{2+}$  ( $^5\text{A}$ ) to 17.86 eV for the vertical ionization  $\text{Fe}(\text{OH})_2^+$  ( $^6\text{A}_1$ )  $\rightarrow$   $\text{Fe}(\text{OH})_2^{2+}$  ( $^5\text{A}'$ ); for the sake of simplicity spin multiplicities are denoted as superscript. Attributing these values to the different features observed experimentally is further complicated by the isobaric interferences apparent in the charge-stripping studies (see above); we will return to these aspects in the Discussion section.

**$(\text{H}_2\text{O})\text{FeOH}^{+/2+}$ .** While the  $(\text{H}_2\text{O})\text{FeOH}^+$  monocation has not been studied previously by theory, the results for the unsolvated  $\text{FeOH}^+$  cation described above imply a quintet ground state of

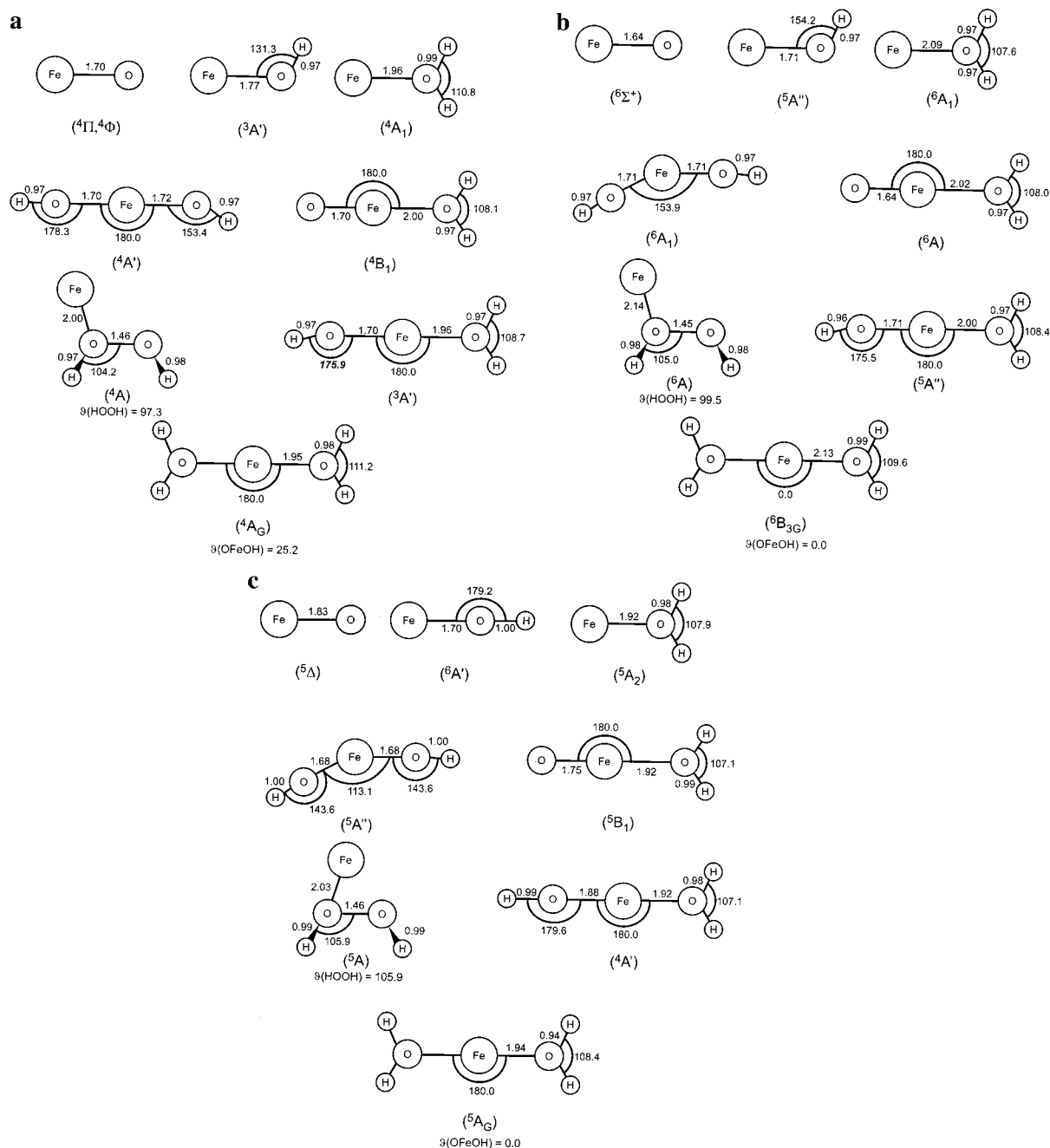


**Figure 2.** B3LYP/6-311+G\* optimized geometries of  $\text{FeO}_m\text{H}_n^{+2+}$  mono- and dications: (a) low-spin monocations, (b) high-spin monocations, and (c) lowest-lying dications; bond lengths in angstroms and angles in degrees.

$(\text{H}_2\text{O})\text{FeOH}^+$ . Indeed, the triplet is much higher in energy (1.83 eV) and not considered any further. Given the small size of the quartet/sixtlet splitting in  $\text{FeOH}^{2+}$ , the presence of an additional water ligand leads us to assume a quartet ground state for the  $(\text{H}_2\text{O})\text{FeOH}^{2+}$  dication, for which the calculations predict  $\text{IE}_{v/a}((\text{H}_2\text{O})\text{FeOH}^+) = 16.07$  eV and  $\text{IE}_a((\text{H}_2\text{O})\text{FeOH}^+) = 15.80$  eV. The energy offset  $\Delta\text{IE}_{v/a} = 0.27$  eV is close to that found for the unsolvated  $\text{FeOH}^{2+}$  dication (0.33 eV). However, unlike the negligible perturbation of the Fe–O bond length upon ionization of  $\text{FeOH}^+$ , the transition  $(\text{H}_2\text{O})\text{FeOH}^+ (^5A'') \rightarrow (\text{H}_2\text{O})\text{FeOH}^{2+} (^4A')$  is associated with a shortening of  $r_{\text{Fe}-\text{O}}$  to the water ligand (from 2.00 to 1.92 Å) and a lengthening of  $r_{\text{Fe}-\text{O}}$  to the hydroxy group (from 1.71 to 1.88 Å). By analogy to the geometry differences in the transition  $\text{Fe}(\text{H}_2\text{O})^+ (^6A_1) \rightarrow \text{Fe}(\text{H}_2\text{O})^{2+} (^5A_2)$ , these effects can tentatively be attributed to the removal of a 4s-type electron in a nonbonding  $\sigma$ -orbital upon ionization of

$(\text{H}_2\text{O})\text{FeOH}^+ (^5A'')$  to the dication, thereby increasing the ion/dipole interaction with water, while simultaneously weakening the Fe–OH bond.

**$\text{Fe}(\text{H}_2\text{O})_2^{+2+}$ .** According to previous ab initio studies, the bisligated monocation  $\text{Fe}(\text{H}_2\text{O})_2^+$  has a  $^4B_{1g}$  ground state.<sup>45</sup> Hence, the ligand field generated by two water molecules favors a low-spin state in the case of  $\text{Fe}(\text{H}_2\text{O})_2^+$ , unlike the sextet ground state of  $\text{Fe}(\text{H}_2\text{O})^+$ . For the dication, a quintet ground state is predicted with  $\text{IE}_v(\text{Fe}(\text{H}_2\text{O})^+) = 12.46$  eV and  $\text{IE}_a(\text{Fe}(\text{H}_2\text{O})^+) = 12.42$  eV. The geometries of the mono- and dications are very similar, and  $\Delta\text{IE}_{v/a}$  amounts to only 0.04 eV.

## Discussion

The measured  $Q_{\text{min}}$  values and the calculated ionization energies are summarized in Table 3. Overall, the agreement

**TABLE 3: Measured  $Q_{\min}$  Values for Charge Stripping of Mass-Selected  $\text{FeO}_m\text{H}_n^+$  Monocations to the Corresponding Dications Using Either the Multiplicative (mult) or Additive (add) Correction Schemes (See Text); Calculated (calc) Vertical and Adiabatic IEs; Other Determinations Included for Comparison; All Data in eV**

	$Q_{\min}(\text{mult})^a$	$Q_{\min}(\text{add})$	$\text{IE}_v(\text{calc})$	$\text{IE}_a(\text{calc})$	other values
$\text{Fe}^+$	$15.39 \pm 0.29$	$15.42 \pm 0.26$	$16.52^b$	$16.52^b$	$16.19^c, 16.3 \pm 0.4^d, 16.6 \pm 0.5^e$
$\text{FeO}^+$	$18.63 \pm 0.30$	$18.10 \pm 0.25$	18.93	18.75	$18.3 \pm 0.3^f$
$\text{FeOH}^+$	$17.30 \pm 0.30$	$17.03 \pm 0.23$	17.23	16.90	$17.0 \pm 0.4^d$
$\text{Fe}(\text{H}_2\text{O})^+$	$14.41 \pm 0.31$	$14.65 \pm 0.30$	$14.04^g$	$13.84^g$	
$[\text{Fe}_2\text{O}_2\text{H}_2]^+$	$13.93 \pm 0.82$	$14.27 \pm 0.63$	<i>h</i>	<i>h</i>	
$(\text{H}_2\text{O})\text{FeOH}^+$	$15.84 \pm 0.41$	$15.81 \pm 0.34$	15.80	16.07	
$\text{Fe}(\text{H}_2\text{O})_2^+$	$12.63 \pm 0.33$	$13.23 \pm 0.25$	12.42	12.46	

<sup>a</sup> The errors are slightly larger than those given in Table 1 because they also include the error of  $\pm 0.14$  eV obtained in repetitive measurements of the toluene calibrant against itself. <sup>b</sup> For the transition  $\text{Fe}^+ (^6\text{D}) \rightarrow \text{Fe}^{2+} (^5\text{D})$ , see text. <sup>c</sup> Spectroscopic value for  $\text{IE}(\text{Fe}^+)$ , ref 25. <sup>d</sup> Previous  $Q_{\min}$  value using the additive calibration scheme and a different ionization technique, ref 14. <sup>e</sup> Previous  $Q_{\min}$  value with ferrocene as precursor, ref 27. <sup>f</sup> Previous  $Q_{\min}$  value using CI of  $\text{Fe}(\text{CO})_5/\text{N}_2\text{O}$  and the multiplicative calibration scheme, ref 2. <sup>g</sup> For the transition  $\text{Fe}(\text{H}_2\text{O})^+ (^6\text{B}_2) \rightarrow \text{Fe}(\text{H}_2\text{O})^{2+} (^5\text{A}_2)$ , see text. <sup>h</sup> See text.

between theory and experiment is pleasing, and we may thus specifically address the different calibration schemes applied in charge-stripping experiments. Large deviations between experiment and theory occur for bare  $\text{Fe}^+$  and  $[\text{Fe}_2\text{O}_2\text{H}_2]^+$ , and in both cases shortcomings of the experimental data are obvious. The former case has been discussed above, and the difference between the measured  $Q_{\min}$  and  $\text{IE}(\text{Fe}^+)$  can be attributed to contribution of electronically excited  $\text{Fe}^+$  to the monocation beam. The  $[\text{Fe}_2\text{O}_2\text{H}_2]^+$  system is rather subtle and deserves discussion in a separate section (see below).

**Calibration Schemes.** The overall agreement observed between experiment and theory allows evaluation of the two different calibrations schemes used in charge-stripping experiments. Calibration is required because of errors in the measurement of the absolute ion kinetic energies in the keV regime and differences in the focusing conditions of mono- and dications in the instrument. It is common to use the transition  $\text{C}_7\text{H}_8^+ \rightarrow \text{C}_7\text{H}_8^{2+}$  of toluene molecular ion as reference, with  $Q_{\min}(\text{C}_7\text{H}_8^+) = 15.7$  eV as an absolute anchor point for calibrating the kinetic energy scale. Therefore, the kinetic energies of toluene mono- and dication,  $E_{\text{kin}}(\text{C}_7\text{H}_8^+)$  and  $E_{\text{kin}}(\text{C}_7\text{H}_8^{2+})$ , are measured and then used to correct those found for the mono- and dication of interest,  $E_{\text{kin}}(\text{M}^+)$  and  $E_{\text{kin}}(\text{M}^{2+})$ . Note that the apparent energy of a dication is  $E_{\text{kin}}(\text{M}^{2+})/2$  because transmission through an electric sector is proportional to the mass-to-charge ratio. In the literature, two different calibration schemes are established.<sup>8</sup> The additivity method assumes that the aberration of the mono- and dication kinetic energies is a constant resulting in  $Q_{\min}(\text{add}) = E_{\text{kin}}(\text{M}^+) - E_{\text{kin}}(\text{M}^{2+}) + \delta$ , where  $\delta = 15.7$  eV  $- [E_{\text{kin}}(\text{C}_7\text{H}_8^+) - E_{\text{kin}}(\text{C}_7\text{H}_8^{2+})]$ . The multiplicative scheme assumes a proportional scaling,  $Q_{\min}(\text{mult}) = [E_{\text{kin}}(\text{M}^+) - E_{\text{kin}}(\text{M}^{2+})]\delta$ , with  $\delta = 15.7$  eV  $/ [E_{\text{kin}}(\text{C}_7\text{H}_8^+) - E_{\text{kin}}(\text{C}_7\text{H}_8^{2+})]$ . By definition, both methods coincide at the  $Q_{\min}$  value of the reference; here,  $Q_{\min}(\text{C}_7\text{H}_8^+) = 15.7$  eV.

Inspection of Table 3 reveals generally better agreement between  $\text{IE}_v(\text{calc})$  and  $Q_{\min}(\text{mult})$  compared to  $\text{IE}_v(\text{calc})$  and  $Q_{\min}(\text{add})$ . Except for  $\text{Fe}^+$  and  $[\text{Fe}_2\text{O}_2\text{H}_2]^+$ , a maximum deviation of 0.37 eV is found between  $\text{IE}_v(\text{calc})$  and  $Q_{\min}(\text{mult})$  of  $\text{Fe}(\text{H}_2\text{O})^+$ , while errors up to 0.8 eV occur between  $\text{IE}_v(\text{calc})$  and  $Q_{\min}(\text{add})$  of  $\text{FeO}^+$ ,  $\text{Fe}(\text{H}_2\text{O})^+$ , and  $\text{Fe}(\text{H}_2\text{O})_2^+$ . Even more instructive is a plot of the difference between the computed  $\text{IE}_v(\text{calc})$  and the measured  $Q_{\min}$  data as a function of  $\text{IE}_v(\text{calc})$ . While the data based on the multiplicative scheme spread around zero, as expected for statistical deviations, the data derived from the additivity scheme show a clear trend to overestimate low and underestimate high  $\text{IE}_v$  (Figure 3). Of course, this analysis relies on the absolute B3LYP results, but the trend of the latter values would only become physically meaningful, if B3LYP

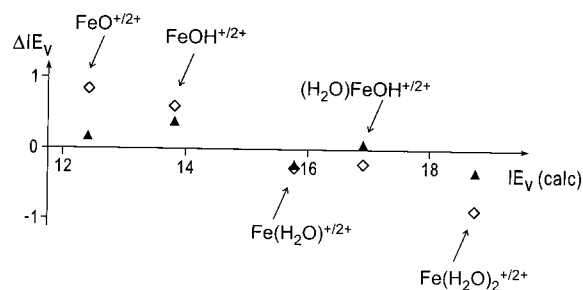


**Figure 3.** Deviations  $\Delta\text{IE}_{\text{mult}} = Q_{\min}(\text{mult}) - \text{IE}_v(\text{calc})$  ( $\blacktriangle$ ) and  $\Delta\text{IE}_{\text{add}} = Q_{\min}(\text{add}) - \text{IE}_v(\text{calc})$  ( $\diamond$ ) as functions of  $\text{IE}_v(\text{calc})$  for  $\text{FeO}^+$ ,  $\text{FeOH}^+$ ,  $\text{Fe}(\text{H}_2\text{O})^+$ ,  $(\text{H}_2\text{O})\text{FeOH}^+$ , and  $\text{Fe}(\text{H}_2\text{O})_2^+$ ; all data in eV.

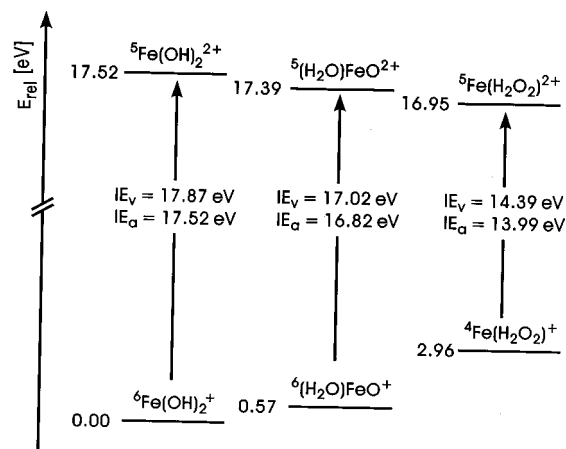


**Figure 4.** Energetics (in eV) of singly and doubly charged  $[\text{Fe}_2\text{O}_2\text{H}_2]^{+2+}$  ions computed at the B3LYP/6-311+G\* level of theory; spin states are indicated as superscripts.

would precisely show the opposite behavior, i.e., a systematic underestimation of low and overestimation of high  $\text{IE}_v$ . As there is no indication to support this assumption,<sup>48</sup> we conclude that at least in the present system the multiplicative correction method is more appropriate.

**$[\text{Fe}_2\text{O}_2\text{H}_2]^{+2+}$ .** Due to the existence of several isomers and the occurrence of isobaric interferences in the experimental studies, the  $[\text{Fe}_2\text{O}_2\text{H}_2]^{+2+}$  system is far from being trivial. Figure 4 gives a schematic survey of the  $[\text{Fe}_2\text{O}_2\text{H}_2]^{+2+}$  isomers of interest here. For each of the monocation isomers (and for each spin state as well), B3LYP predicts different  $\text{IE}_v$  and  $\text{IE}_a$ . If we assume that CI of  $\text{Fe}(\text{CO})_5/\text{N}_2\text{O}/\text{H}_2\text{O}$  leads to the generation of ground-state  $\text{Fe}(\text{OH})_2^+$  as the most stable monocationic species, a  $Q_{\min}$  value of 17.87 eV is expected from the computed  $\text{IE}_v$ . However, the precursor mixture used in CI also implies the generation of  $(\text{H}_2\text{O})\text{FeO}^+$  via the association reaction 4. For this isomer, the calculations predict a somewhat lower

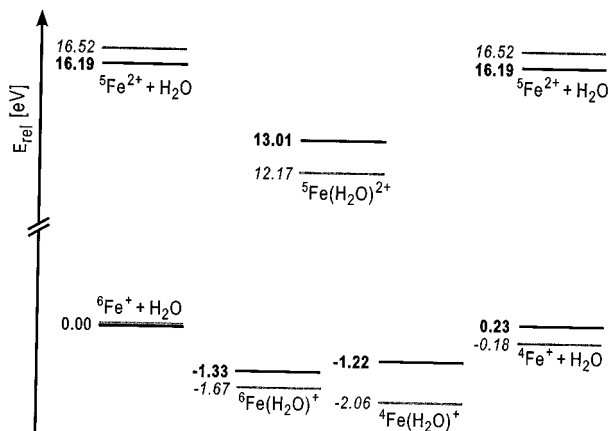


**Figure 5.** Energetics (in eV) of singly and doubly charged  $\text{Fe}(\text{H}_2\text{O})_2^{2+}$  computed at the B3LYP/6-311+G\* level of theory (gray lines, italic figures) and the ‘best estimates’ based on literature data (black lines, bold figures); spin states are indicated as superscripts.

$Q_{\min}$  value of only 17.02 eV. Although it appears unlikely, small amounts of  $\text{Fe}(\text{H}_2\text{O})_2^+$  might be generated in the ion source and contribute to the  $Q_{\min}$  measurements because ionization energies of only about 14 eV are predicted for the different spin states. While this situation is already quite complex, also a nonnegligible interference of  $[\text{Fe}, \text{O}_2, \text{H}_2]^+$  by  $^{54}\text{Fe}(\text{H}_2\text{O})_2^+$  is apparent in the experimental study

Qualitatively, we can attribute the low- and high-energy components of the charge-stripping peak shown in the upper trace of Figure 1 to  $^{54}\text{Fe}(\text{H}_2\text{O})_2^+$  giving rise to the onset of the CS peak at about 12 eV and  $\text{Fe}(\text{OH})_2^+$  leading to the high-energy tail between 17 and 20 eV. The central component, also giving rise to the peak maximum at ca. 16 eV, is of unknown origin. Using the dication signal of  $\text{Fe}(\text{H}_2\text{O})_2^+$  (lower trace of Figure 1) as a reference, the shape of the dication signal in the upper trace can indeed be modeled assuming three different components. However, several assumptions are required in this procedure; in particular it is obvious that also more than three components can contribute. In view of the ambiguities associated with such a deconvolution of overlapping features, we refrain from a quantitative analysis of the experimental data. Anyhow, it is apparent that the  $Q_{\min}$  values given in Tables 1 and 2 do not reflect meaningful quantities for any of the species involved because noncomposite charge-stripping signals are assumed in the threshold analysis. Thus, for the time being we are left with referring to the computational predictions in the subsequent analysis of the dication properties.

**Best Estimates.** In this section, let us critically review the experimental and theoretical data in order to determine best estimates for the ionization energies of the  $\text{FeO}_m\text{H}_n^+$  cations as a basis for the further evaluation of the thermochemistry of the  $\text{FeO}_m\text{H}_n^{2+}$  dications. This procedure includes an evaluation of errors and limitation of the data to the significant digits. As far as the conversion of  $Q_{\min}$  values to  $\text{IE}_a$  is concerned, we add an error of  $\pm 0.1$  eV to the experimental data in order to account for uncertainties in  $\Delta\text{IE}_{v/a}$  and effects of vibrational progression in the transition from mono- to dications.<sup>14</sup> Based on the evaluation of the two calibration schemes (see above), we refer to the multiplicative  $Q_{\min}$  values throughout.

In the case of bare  $\text{Fe}^+$ , we simply adopt the spectroscopic value  $\text{IE}(\text{Fe}^+) = 16.1879 \pm 0.0012$  eV.<sup>25</sup> Next,  $\text{IE}_a(\text{FeO}^+) = 18.3 \pm 0.4$  eV and  $\text{IE}(\text{FeOH}^+) = 17.0 \pm 0.4$  eV are derived from the different sets of experimental data given in Table 2 in conjunction with the calculated  $\Delta\text{IE}_{v/a}$ . For  $\text{Fe}(\text{H}_2\text{O})_2^+$ , the conversion of  $Q_{\min}$  to  $\text{IE}_a$  is more problematic (Figure 5). B3LYP

**TABLE 4: Best Estimates of  $\text{IE}_a(\text{FeO}_m\text{H}_n^+)$  and Derived Heats of Formation ( $\Delta_f H_{0\text{K}}$ ) and Low-Lying Charge Separation Limits ( $\Delta E_{\text{sep}}$  with Monocation Fragments Indicated) of the Corresponding  $\text{FeO}_m\text{H}_n^{2+}$  Dications as Well as Proton Affinities (PA)<sup>a</sup> of the Related Monocations  $\text{FeO}_m\text{H}_{(n-1)}^+$ ; All Data in eV<sup>b</sup>**

	$\text{IE}_a(\text{M}^+)^c$	$\Delta_f H_{0\text{K}}(\text{M}^{2+})$	$\Delta E_{\text{sep}}$	PA
Fe	16.19	28.4		
FeO	$18.3 \pm 0.4$	29.6	-1.2 ( $\text{Fe}^+ + \text{O}^+$ )	
FeOH	$17.0 \pm 0.4$	25.8	-4.5 ( $\text{Fe}^+ + \text{OH}^+$ )	1.4
$\text{Fe}(\text{H}_2\text{O})$	$14.3 \pm 0.5$	22.7	-0.4 ( $\text{Fe}^+ + \text{H}_2\text{O}$ )	2.0
$\text{Fe}(\text{OH})_2$	$17.5 \pm 0.5$	23.4	-1.2 ( $\text{FeOH}^+ + \text{OH}^+$ )	1.1
$(\text{H}_2\text{O})\text{FeO}$	$16.8 \pm 0.5$	23.3	-1.8 ( $\text{FeO}^+ + \text{H}_2\text{O}^+$ )	$1.2^d$
$(\text{H}_2\text{O})\text{FeOH}$	$15.6 \pm 0.5$	19.6	-0.7 ( $\text{FeOH}^+ + \text{H}_2\text{O}^+$ )	$2.2^e$
			-2.1 ( $\text{FeO}^+ + \text{H}_3\text{O}^+$ )	$1.7^f$
$\text{Fe}(\text{H}_2\text{O})_2$	$12.6 \pm 0.4$	16.8	+1.7 ( $\text{Fe}(\text{H}_2\text{O})^+ + \text{H}_2\text{O}^+$ )	3.0
			-1.8 ( $\text{FeOH}^+ + \text{H}_3\text{O}^+$ )	

<sup>a</sup> Not defined for  $\text{Fe}^+$  and  $\text{FeO}^+$ . <sup>b</sup> For the derived values, the errors are equal or even exceed those of the  $\text{IE}_a$  data, but are omitted for the sake of clarity. <sup>c</sup> Best estimates, see text. <sup>d</sup> Using  $\Delta_f H_{0\text{K}}(\text{OFeOH}^+) = 8.6 \pm 0.5$  eV. <sup>e</sup> Referring to  $\text{Fe}(\text{OH})_2^+$ . <sup>f</sup> Referring to  $(\text{H}_2\text{O})\text{FeO}^+$ .

predicts a wrong order of states for the monocations together with different  $\Delta\text{IE}_{v/a}$  for both. Hence, depending on the choice of the reference state, different corrections need to be applied. For example, if we would assume that only the sextet ground state of  $\text{Fe}(\text{H}_2\text{O})^+$  is formed upon CI, the measured  $Q_{\min} = 14.41 \pm 0.31$  eV would yield  $\text{IE}_a = 14.21$  eV. Instead,  $\Delta\text{IE}_{v/a}$  is negligible for the quartet monocation, suggesting  $\text{IE}_a = 14.38$  eV for  $\text{Fe}(\text{H}_2\text{O})^+$  ( $^4\text{A}_2$ ); the latter value changes to  $\text{IE}_a = 14.26$  eV if referring to the  $\text{Fe}(\text{H}_2\text{O})^+$  ( $^6\text{A}_1$ ) ground state predicted in CCSD(T) calculations.<sup>35</sup> Due to these ambiguities, we increase the error margin of the correction by  $\pm 0.1$  eV and arrive at a best estimate of  $\text{IE}_a(\text{Fe}(\text{H}_2\text{O})^+) = 14.3 \pm 0.5$  eV. As mentioned above, we must rely on the computational data for the  $[\text{Fe}, \text{O}_2, \text{H}_2]^+$  system, which predict  $\text{IE}_a(\text{Fe}(\text{OH})_2^+) = 17.5 \pm 0.5$  eV and  $\text{IE}_a((\text{H}_2\text{O})\text{FeO}^+) = 16.8 \pm 0.5$  eV; the error estimate is derived from the accuracy of the other predictions. Using similar considerations as for  $\text{FeO}^+$  and  $\text{FeOH}^+$ ,  $\text{IE}((\text{H}_2\text{O})\text{FeOH}^+) = 15.6 \pm 0.5$  eV and  $\text{IE}(\text{Fe}(\text{H}_2\text{O})_2^+) = 12.6 \pm 0.4$  eV are obtained for the two remaining species. With respect to the multiplicative calibration schemes, the absolute dication energetics predicted by B3LYP are consistent within the  $\pm 0.5$  eV error estimate associated with this level of theory; not unexpectedly, the bare metal atom shows the largest deviation.<sup>16,42</sup>

### Dication Thermochemistry

Based upon the best estimates derived above and complementary literature data of the neutral and cationic species, the heats of formation ( $\Delta_f H_{0\text{K}}$ ) of the dications are displayed in Table 4. Subsequently, the entire thermochemistry of the dications under study can be evaluated using Born–Haber cycles.<sup>2,10,14</sup>

A property of particular relevance for dications is their thermochemical stability in the gas phase, i.e., the energetic location of the dication minimum relative to possible charge separation asymptotes yielding two singly charged fragments (“Coulomb explosion”). Thus, if the dication is lower in energy than the lowest lying charge-separation fragment ( $\Delta E_{\text{sep}} > 0$ ), the dication is termed thermochemically stable in the gas phase.<sup>7</sup> If  $\Delta E_{\text{sep}} < 0$ , the dications are metastable with respect to charge separation, provided dissociation is hindered by barriers.<sup>6–8</sup> Except  $\text{Fe}(\text{H}_2\text{O})_2^{2+}$ , however, charge separations via direct Fe–O cleavages to the corresponding monocationic fragments are exothermic for all  $\text{FeO}_m\text{H}_n^{2+}$  dications under study. Even though  $\text{IE}_a(\text{Fe}(\text{H}_2\text{O})^+)$  is almost 2 eV lower than  $\text{IE}(\text{Fe}^+)$ , charge separation to afford  $\text{Fe}^+ + \text{H}_2\text{O}^+$  is still slightly exothermic. In



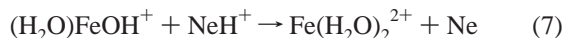
**TABLE 5: Fe–O Bond Strengths in  $\text{FeO}_m\text{H}_n^{+/2+}$  Mono- and Dications (in eV) and Formal Valencies<sup>a</sup> of the Iron Atom**

Fe–O		$D_0$	Fe–OH		$D_0$	Fe–OH <sub>2</sub>		$D_0$
(H <sub>2</sub> O)Fe <sup>+</sup> –O	III <sub>solv</sub>	4.5 <sup>b</sup>	(H <sub>2</sub> O)Fe <sup>+</sup> –OH	II <sub>solv</sub>	4.8 <sup>b</sup>	(H <sub>2</sub> O)Fe <sup>+</sup> –OH <sub>2</sub>	I <sub>solv</sub>	1.7 <sup>c</sup>
Fe <sup>+</sup> –O	III	3.5 <sup>c</sup>	Fe <sup>+</sup> –OH	II	3.8 <sup>c</sup>	Fe <sup>+</sup> –OH <sub>2</sub>	I	1.3 <sup>c</sup>
(H <sub>2</sub> O)Fe <sup>2+</sup> –O	IV <sub>solv</sub>	2.0	(H <sub>2</sub> O)Fe <sup>2+</sup> –OH	III <sub>solv</sub>	3.5	(H <sub>2</sub> O)Fe <sup>2+</sup> –OH <sub>2</sub>	II <sub>solv</sub>	3.4
Fe <sup>2+</sup> –O	IV	1.4	HOFe <sup>+</sup> –OH	III	3.3	HOFe <sup>+</sup> –OH <sub>2</sub>	II	2.3 <sup>b</sup>
			Fe <sup>2+</sup> –OH	III	3.0	Fe <sup>2+</sup> –OH <sub>2</sub>	II	3.2
			HOFe <sup>2+</sup> –OH	IV	2.8	OFe <sup>+</sup> –OH <sub>2</sub>	III	2.3 <sup>b</sup>
						HOFe <sup>2+</sup> –OH <sub>2</sub>	III	3.7
						OFe <sup>2+</sup> –OH <sub>2</sub>	IV	3.8

<sup>a</sup> The formal oxidation states of iron are given in roman numerals; see text for definition. <sup>b</sup> Taken from ref 9. <sup>c</sup> Taken from ref 20.

contrast, for the bisligated  $\text{Fe}(\text{H}_2\text{O})_2^{2+}$  complex direct Fe–O cleavage to the charge-separated products  $\text{Fe}(\text{H}_2\text{O})^+ + \text{H}_2\text{O}^+$  is indeed endothermic by 1.7 eV, but facile proton migration from one to the other water ligand<sup>49</sup> provides access to the  $\text{FeOH}^+ + \text{H}_3\text{O}^+$  asymptote which is still 1.8 eV lower in energy than the dication minimum. Thus, none of the  $\text{FeO}_m\text{H}_n^{2+}$  dications studied here is thermochemically stable.

The last process considered, i.e., the charge separation  $\text{Fe}(\text{H}_2\text{O})_2^{2+} \rightarrow \text{FeOH}^+ + \text{H}_3\text{O}^+$ , leads us directly to a second peculiar question in the chemistry of dications, i.e., the proton affinities (PAs) of the corresponding monocations. In conjunction with complementary thermochemical data, the heats of formation given in Table 4 can be used to evaluate these figures. For example, the comparison of  $\Delta_f H_{0\text{K}}(\text{FeOH}^{2+}) = 25.8$  eV with  $\Delta_f H_{0\text{K}}(\text{FeO}^+) = 11.3$  eV and  $\Delta_f H_{0\text{K}}(\text{H}^+) = 15.9$  eV implies a proton affinity of 1.4 eV for the  $\text{FeO}^+$  monocation. Thus, diatomic  $\text{FeO}^+$  is a monocation having a positive proton affinity. Similarly,  $\text{FeOH}^+$ ,  $\text{OFeOH}^+$ ,  $\text{Fe}(\text{OH})_2^+$ ,  $(\text{H}_2\text{O})\text{FeO}^+$ , and  $(\text{H}_2\text{O})\text{FeOH}^+$  bear positive PAs. While most of these monocation PAs are small compared to that of typical neutral molecules, the considerable  $\text{PA}((\text{H}_2\text{O})\text{FeOH}^+) = 3.0$  eV suggests that cation/cation reactions are conceivable in which proton transfer from a monocation to another one yields a dication concomitant with a neutral species. For example, the hypothetical protonation of  $(\text{H}_2\text{O})\text{FeOH}^+$  by the protonated rare gas  $\text{NeH}^+$  according to reaction 7 is exothermic by 1.0 eV.



Of course, protonation of a cation is hindered by a considerable barrier due to Coulomb repulsion of the monocationic reactants. Despite its exothermicity, reaction 7 is therefore not expected to occur at room temperature. However, the occurrence of cation/cation reactions — even at elevated energies — offers an interesting perspective for gas-phase ion chemistry and physics.<sup>7</sup>

Let us now turn to some properties of the various  $\text{FeO}_m\text{H}_n^{+/2+}$  species as functions of formal valence state and of ligation. The first systematic charge-stripping studies of ligated transition metal ions are due to Lebrilla and co-workers.<sup>14,50,51</sup> However, these investigations were mostly focused on the variation of the metal while keeping the ligand fixed. Instead, our results on the dication energetics for a single metal, i.e., selected  $\text{FeO}_m\text{H}_n^{2+}$  dications, permit a more detailed analysis of the effect of ligation on dication energetics of iron compounds. In particular, the influence of the formal valence on the bond strengths as well as the role of water as a solvating ligand is addressed.

Table 5 displays the Fe–O bond dissociation energies ( $D_0$ ) of the  $\text{FeO}_m\text{H}_n^{+/2+}$  mono- and dications under study together with the formal valencies of iron given in roman numerals. Here, the oxo and hydroxy ligands are considered as strict two- and one-electron acceptors, i.e.,  $\text{O}^{2-}$  and  $\text{HO}^-$ , respectively, and the

positive charges are counted as extra valencies. While  $\text{H}_2\text{O}$  ligands do not affect the oxidation state, the presence of these solvating ligands is indicated by a subscript. For example,  $\text{FeO}^+$  monocation and  $\text{FeOH}^{2+}$  dication are formal Fe(III) compounds,  $(\text{H}_2\text{O})\text{FeO}^+$  is Fe(III<sub>solv</sub>), etc. According to this formalism, both  $D_0(\text{Fe}^{+/2+}-\text{O})$  and  $D_0(\text{Fe}^{+/2+}-\text{OH})$  show clear trends toward decreasing dissociation energies with increasing valence of iron. These observations are consistent with the redox chemistry of iron in solution where Fe(II) and Fe(III) are favored over all other oxidation states. Further, solvation of the metal by a water ligand is found to significantly increase the respective  $\text{Fe}^{+/2+}-\text{O}$  and  $\text{Fe}^{+/2+}-\text{OH}$  bonds strengths, which is consistent with a stabilization of the polar, covalent bonds to the oxo and hydroxy ligands in the presence of an additional ligand. Instead,  $D_0(\text{Fe}^{+/2+}-\text{OH}_2)$  does not correlate with the formal oxidation state, but rather increases with net charge. This is consistent with the description of the binding to the water ligand as a primarily electrostatic interaction. Differential stabilization of the dications by the water ligands, i.e.,  $\Delta I E_{\text{solv}} = I E_{\text{a}}(\text{M}^+) - I E_{\text{a}}((\text{H}_2\text{O})\text{M}^+)$ , amounts to 1.9 eV for  $\text{Fe}^+/\text{Fe}(\text{H}_2\text{O})^+$ , 1.5 eV for  $\text{FeO}^+/\text{Fe}(\text{H}_2\text{O})\text{FeO}^+$ , 1.4 eV for  $\text{FeOH}^+/\text{Fe}(\text{H}_2\text{O})\text{FeOH}^+$ , and 1.7 eV for  $\text{Fe}(\text{H}_2\text{O})^+/\text{Fe}(\text{H}_2\text{O})_2^+$ . These values are quite similar (average  $\Delta I E_{\text{solv}} = 1.6 \pm 0.3$  eV) and close to the mere ion–dipole interaction of 1.5 eV for water and a positive charge at a distance of ca. 1.9 Å. Hence, the differential stabilization of the hydrated iron dications can by and large be attributed to electrostatic forces.

## Conclusions

Charge-stripping mass spectrometry in conjunction with theoretical studies can be used to assess the energetics of  $\text{FeO}_m\text{H}_n^{2+}$  dications. Given the error limits of the different approaches, the agreement between experiment and theory is reasonably good. In fact, the theoretical predictions assist to trace the origin of the discrepancies due to interferences of excited electronic states or isobaric ions. Further, the present results indicate that the multiplicative calibration scheme is more appropriate for correction of the charge-stripping data.

Evaluation of the dication energetics via Born–Haber cycles allows analysis of some of the dication thermochemical properties. None of the  $\text{FeO}_m\text{H}_n^{2+}$  dications studied is thermochemically stable as in all cases lower lying charge-separation asymptotes exist. With respect to bond strengths in the mono- and dications, the  $\text{Fe}^{+/2+}-\text{O}$  and  $\text{Fe}^{+/2+}-\text{OH}$  bonds show clear dependencies of the formal valence of iron and decrease with increasing oxidation state, whereas the interaction with water is dominated by the net charge and is primarily electrostatic. Finally, these data allow assessment of the ion thermochemistry of iron oxides and hydroxides in the gas phase, which might be of relevance in modeling the role of these iron compounds in the atmospheric chemistry and in corrosion phenomena.

**Acknowledgment.** Continuous financial support by the Deutsche Forschungsgemeinschaft, the Fonds der Chemischen

Industrie, the Volkswagen-Stiftung, and the Gesellschaft von Freunden der Technischen Universität Berlin is gratefully acknowledged. We thank Dr. Ilona Kretzschmar for helpful discussions and are grateful to the Konrad-Zuse-Zentrum Berlin for the generous allocation of computer time. Dr. R. Dressler is acknowledged for a preprint of ref 5.

## References and Notes

- (1) Schröder, D.; Fiedler, A.; Schwarz, J.; Schwarz, H. *Inorg. Chem.* **1994**, *33*, 5094.
- (2) Harvey, J. N.; Heinemann, C.; Fiedler, A.; Schröder, D.; Schwarz, H. *Chem. Eur. J.* **1996**, *2*, 1230.
- (3) Brönstrup, M.; Schröder, D.; Schwarz, H. *Chem. Eur. J.* **1999**, *5*, 1176.
- (4) Jacobsen, F. Holcman, J.; Sehested, K. *Int. J. Chem. Kinet.* **1998**, *30*, 215.
- (5) Dressler, R. In *Chemistry in Extreme Environments*; Ng, C. Y., Dressler, R., Eds.; Phys. Chem. Ser., Singapore, in preparation.
- (6) Veký, K. *Mass Spectrom. Rev.* **1995**, *14*, 195.
- (7) Schröder, D.; Schwarz, H. *J. Phys. Chem. A* **1999**, *103*, 7385.
- (8) Lammertsma, K.; Schleyer, P. v. R.; Schwarz, H. *Angew. Chem., Int. Ed. Engl.* **1989**, *28*, 1321.
- (9) Bärsch, S.; Schröder, D.; Schwarz, H. *Chem. Eur. J.*, in print.
- (10) Schröder, D.; Bärsch, S.; Schwarz, H. *Int. J. Mass Spectrom. Ion Processes* **1999**, *192*, 125.
- (11) Schalley, C. A.; Schröder, D.; Schwarz, H. *Int. J. Mass Spectrom. Ion Processes* **1996**, *153*, 173.
- (12) Schröder, D.; Schwarz, H. *Int. J. Mass Spectrom. Ion Processes* **1995**, *146/147*, 183.
- (13) The onsets have been determined using procedures described in detail previously (ref 8). For an example of an application to metal-ion chemistry see ref 14.
- (14) McCullough-Catalano, S.; Lebrilla, C. B. *J. Am. Chem. Soc.* **1993**, *115*, 1441.
- (15) Frisch, M. J.; Trucks, G. W.; Schlegel, H. B.; Gill, P. M. W.; Johnson, B. G.; Robb, M. A.; Cheeseman, J. R.; Keith, T.; Petersson, G. A.; Montgomery, J. A.; Raghavachari, K.; Al-Laham, M. A.; Zakrzewski, V. G.; Ortiz, J. V.; Foresman, J. B.; Peng, C. Y.; Ayala, P. Y.; Chen, W.; Wong, M. W.; Andres, J. L.; Replogle, E. S.; Gomperts, R.; Martin, R. L.; Fox, D. J.; Binkley, J. S.; Defrees, D. J.; Baker, J.; Stewart, J. P.; Head-Gordon, M.; Gonzalez, C.; Pople, J. A. *Gaussian 94*, Revision B.3; Gaussian, Inc.: Pittsburgh, PA, 1995.
- (16) Glukhovtsev, M. N.; Bach, R. D.; Nagel, C. J. *J. Phys. Chem. A* **1997**, *101*, 316.
- (17) Kappes, M. M.; Staley, R. H. *J. Am. Chem. Soc.* **1981**, *103*, 1286.
- (18) Unless mentioned otherwise, auxiliary thermochemical data are taken from ref 19 (for nonmetal species) and ref 20 (for gaseous iron compounds).
- (19) Lias, S. G.; Bartmess, J. E.; Liebman, J. F.; Holmes, J. L.; Levin, R. D.; Mallard, W. G. *Gas Phase Ion and Neutral Thermochemistry. J. Phys. Chem. Ref. Data* **1988**, *17*, Suppl. 1.
- (20) Armentrout, P. B.; Kickel, B. L. In *Organometallic Ion Chemistry*; Kluwer: Dordrecht, 1996; p 1.
- (21) Foster, M. S.; Beauchamp, J. L. *J. Am. Chem. Soc.* **1975**, *97*, 4808.
- (22) Dalleska, N. F.; Honma, K.; Sunderlin, L. S.; Armentrout, P. B. *J. Am. Chem. Soc.* **1994**, *116*, 3519.
- (23) Baranov, V.; Javahery, G.; Hopkinson, A. C.; Bohme, D. K. *J. Am. Chem. Soc.* **1995**, *117*, 12801.
- (24) Schröder, D.; Schwarz, H. *Angew. Chem.* **1990**, *102*, 1466; *Angew. Chem., Int. Ed. Engl.* **1990**, *29*, 1431.
- (25) Sugar, J.; Corliss, C. *J. Phys. Chem. Ref. Data* **1985**, *14*, Suppl. 2.
- (26) Kemper, P. R.; Bowers, M. T. *J. Phys. Chem.* **1991**, *95*, 5134, and references therein.
- (27) Rabrenovic, M.; Ast, T.; Beynon, J. H. *Int. J. Mass Spectrom. Ion Processes* **1984**, *61*, 31.
- (28) Porter, C. J.; Proctor, C. J.; Ast, T.; Beynon, J. H. *Int. J. Mass Spectrom. Ion Phys.* **1982**, *41*, 265.
- (29) Guilhaus, M.; Kingston, R. G.; Brenton, A. G.; Beynon, J. H. *Int. J. Mass Spectrom. Ion Processes* **1985**, *63*, 101.
- (30) Heinemann, C.; Schröder, D.; Schwarz, H. *J. Phys. Chem.* **1995**, *99*, 16195, and references therein.
- (31) Compared to our work reported in ref 2, we have meanwhile also refined our strategy in raw-data acquisition and handling in the determination of  $Q_{\min}$  values.
- (32) Schröder, D.; Fiedler, A.; Hrušák, J.; Schwarz, H. *J. Am. Chem. Soc.* **1992**, *114*, 1215.
- (33) Fiedler, A.; Hrušák, J.; Koch, W.; Schwarz, H. *Chem. Phys. Lett.* **1993**, *211*, 242.
- (34) Filatov, M.; Shaik, S. *J. Phys. Chem. A* **1998**, *102*, 3835.
- (35) Irigoias, A.; Fowler, J. E.; Ugalde, J. M. *J. Am. Chem. Soc.* **1999**, *121*, 1, 8549.
- (36) Cooks, R. G.; Ast, T.; Beynon, J. H. *Int. J. Mass Spectrom. Ion Phys.* **1973**, *11*, 490.
- (37) Holthausen, M. C.; Heinemann, C.; Cornehl, H. H.; Koch, W.; Schwarz, H. *J. Chem. Phys.* **1995**, *102*, 4931.
- (38) Holthausen, M. C.; Mohr, M.; Koch, W. *Chem. Phys. Lett.* **1995**, *240*, 245.
- (39) Blomberg, M. R. A.; Siegbahn, P. E. M.; Svensson, M. *J. Chem. Phys.* **1996**, *104*, 9546.
- (40) Bach, R. D.; Shobe, D. S.; Schlegel, H. B.; Nagel, C. J. *J. Phys. Chem.* **1996**, *100*, 8770.
- (41) Kellogg, C. B.; Irikura, K. K. *J. Phys. Chem. A* **1999**, *103*, 1150.
- (42) Sodupe, M.; Branchadell, V.; Rosi, M.; Bauschlicher, C. W., Jr. *J. Phys. Chem. A* **1997**, *101*, 7854.
- (43) Yoshizawa, K.; Shiota, Y.; Yamabe, T. *Organometallics* **1998**, *17*, 2825.
- (44) Husband, J.; Aguirre, F.; Ferguson, P.; Metz, R. *J. Chem. Phys.* **1999**, *111*, 1433.
- (45) Rosi, M.; Bauschlicher, C. W., Jr. *J. Chem. Phys.* **1990**, *92*, 1876.
- (46) Similarly, high-spin ground states were reported for the metal dihydroxide monocations  $\text{Co}(\text{OH})_2^+$  and  $\text{Ni}(\text{OH})_2^+$ ; see: Ricca, A.; Bauschlicher, C. W. *J. Phys. Chem. A* **1997**, *101*, 8949.
- (47) Schalley, C. A.; Wesendrup, R.; Schröder, D.; Schwarz, H. *Organometallics* **1996**, *15*, 678.
- (48) Although no systematic studies have been performed so far, B3LYP calculations have provided reasonably accurate results for various types of dications. For recent examples, see: (a) Hrušák, J.; Herman, Z.; Iwata, S. *Int. J. Mass Spectrom.* **1999**, *192*, 165. (b) Petrie, S.; Radom, L. *Int. J. Mass Spectrom.* **1999**, *192*, 173.
- (49) For related examples of proton migration in hydrated metal ions and further references on this topic, see: Beyer, M.; Williams, E. R.; Bondybey, V. E. *J. Am. Chem. Soc.* **1999**, *121*, 1565.
- (50) McCullough, S. M.; Jones, A. D.; Lebrilla, C. B. *Int. J. Mass Spectrom. Ion Processes* **1991**, *107*, 545.
- (51) Dai, P.; McCullough-Catalano, S.; Boulton, M.; Jones, A. D.; Lebrilla, C. B. *Int. J. Mass Spectrom. Ion Processes* **1995**, *144*, 67.